Volume 1, Number 2

JPCR | JOURNAL OF PEDIATRIC CASE REPORTS

A MULTIDISCIPLINARY JOURNAL OF CASE REPORTS

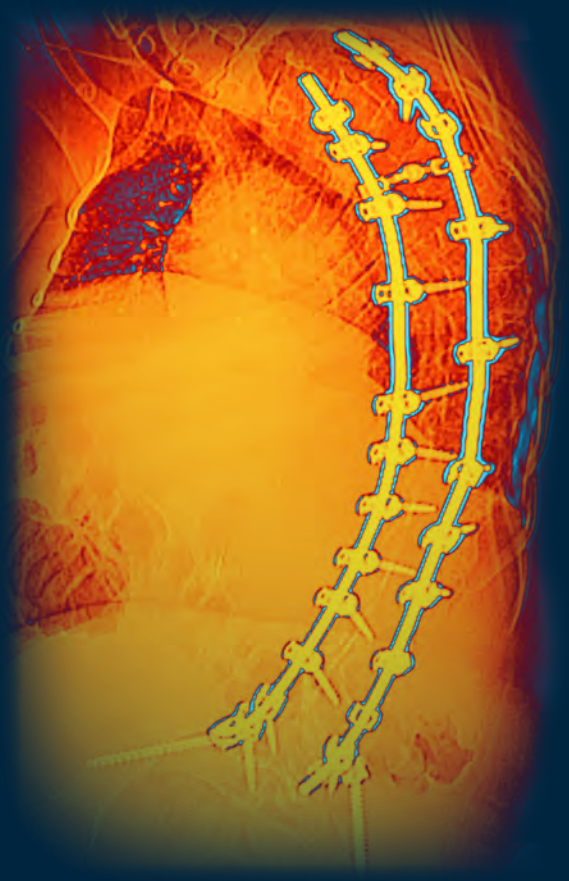

Spinal Muscular Atrophy

Clubfoot

Neutropenic Colitis

Slipped Capital Femoral Epiphysis

Pectus Excavatum

Fibrosing Mediastinitis

www.journalofpediatriccasereports.com

JPCR | JOURNAL OF PEDIATRIC CASE REPORTS

A MULTIDISCIPLINARY JOURNAL OF CASE REPORTS

Anderson Publishing, Ltd
180 Glenside Avenue,
Scotch Plains, NJ 07076
Tel: 908-271-8644

VOLUME 1 NUMBER 2

Spinal Muscular Atrophy

Janki Desai, BS; Richard B. Towbin, MD; Carrie M. Schaefer, MD; Alexander J. Towbin, MD

Abstract

Spinal muscular atrophy (SMA) is an inherited neuromuscular disorder characterized by progressive muscle weakness. It has varying clinical severity, ranging from mild proximal muscle weakness to death from restrictive lung disease. The diagnosis is confirmed by genetic testing. Treatment includes survival motor neuron (SMN2) splicing modulator nusinersen, which may be challenging to administer intrathecally as patients develop varying degrees of scoliosis over time, making midline or paramedian lumbar punctures difficult. Patients with complex spinal anatomy may benefit from preprocedural and intraprocedural imaging to allow for a transforaminal approach for the intrathecal administration of nusinersen. Additional SMA treatments include risdiplam, a newer, oral splicing modulator, or SMN1 gene replacement therapy with Zolgensma.

Keywords: neuromuscular, spine, congenital

Case Summary

A 21-year-old man with type 1 spinal muscular atrophy (SMA) presented with initial onset of symptoms at 5 months of age, including delayed milestones and the inability to sit independently. The diagnosis was confirmed by genetic testing, with no copies of the survival motor neuron 1 (SMN1) gene and 3 copies of the SMN2 gene. The expanded Hammersmith Functional Motor Scale score is 0, and the Revised Upper Limb Module for SMA is 1. Additionally, he is ventilator dependent and requires BiPAP at night. Spinal fixation from C4 to S1 was performed for severe levoscoliosis. He began intrathecal (IT) nusinersen (Biogen, Cambridge, Massachusetts) at 17 years of age. Since beginning the IT nusinersen, he has greater hand movement and an improvement in his voice quality.

Imaging Findings

Figure 1. Scout image of a CT of the spine demonstrating the presence of a severe levoconvex rotary scoliosis of the thoracolumbar spine with spinal fixation.

Figure 2A-C. 2A) CT axial image of the lumbar spine demonstrating planned left transforaminal access (blue arrow) for intrathecal nusinersen administration, 2B) Lateral fluoroscopic view of the lumbar spine with the spinal needle (blue arrow) entering the inferior-most aspect of the neural foramen for IT nusinersen, to avoid the neurovascular bundle in the upper 2/3 of the foramen, and 2C) Frontal fluoroscopic image demonstrating that the spinal needle tip (blue arrow) is near the midline of the thecal sac.

Figure 3. C1-2 puncture.

Figure 1. Scout image of a CT of the spine demonstrating the presence of a severe levoconvex rotary scoliosis of the thoracolumbar spine with spinal fixation.

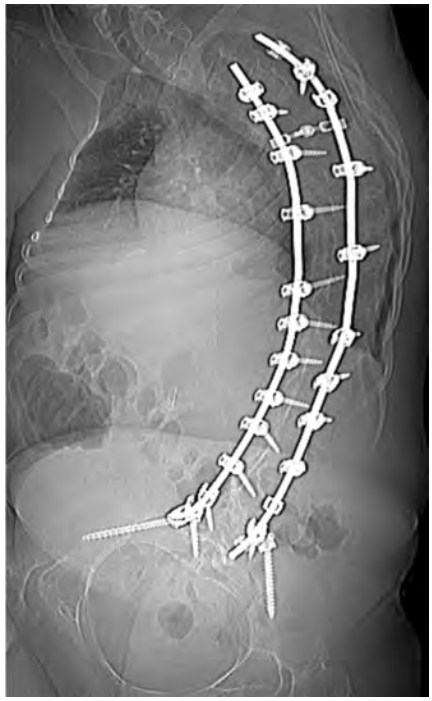

Diagnosis

SMA.

The differential diagnosis of SMA is extensive and includes many conditions

Affiliations: University of Arizona College of Medicine-Phoenix, Phoenix, Arizona (Desai); Department of Radiology, Phoenix Children's Hospital, Phoenix, Arizona (RB Towbin, Schaefer); Department of Radiology, Cincinnati Children's Hospital, University of Cincinnati College of Medicine, Cincinnati, Ohio (AJ Towbin).
Disclosures: The authors have no conflicts of interest to disclose. None of the authors received outside funding for the production of this original manuscript and no part of this article has been previously published elsewhere.

https://doi.org/10.37549/JPCR-26-0082

Figure 2. (A) CT axial image of the lumbar spine demonstrating planned left transforaminal access (blue arrow) for intrathecal (IT) nusinersen administration. 1) Segmental spinal nerve/dorsal root ganglion, 2) Sinuvertebral nerves and rami communicantes, 3) spinal branch of segmental arteries, 4) intervertebral veins. (B) Lateral fluoroscopic view of the lumbar spine with the spinal needle (blue arrow) entering the inferior-most aspect of the neural foramen for IT nusinersen, to avoid the neurovascular bundle in the upper 2/3 of the foramen. (C) Frontal fluoroscopic image demonstrating that the spinal needle tip (blue arrow) is near the midline of the thecal sac. (D,E) showing the needle in the inferior aspect of the neuroforamina with the needle tipin the midline.

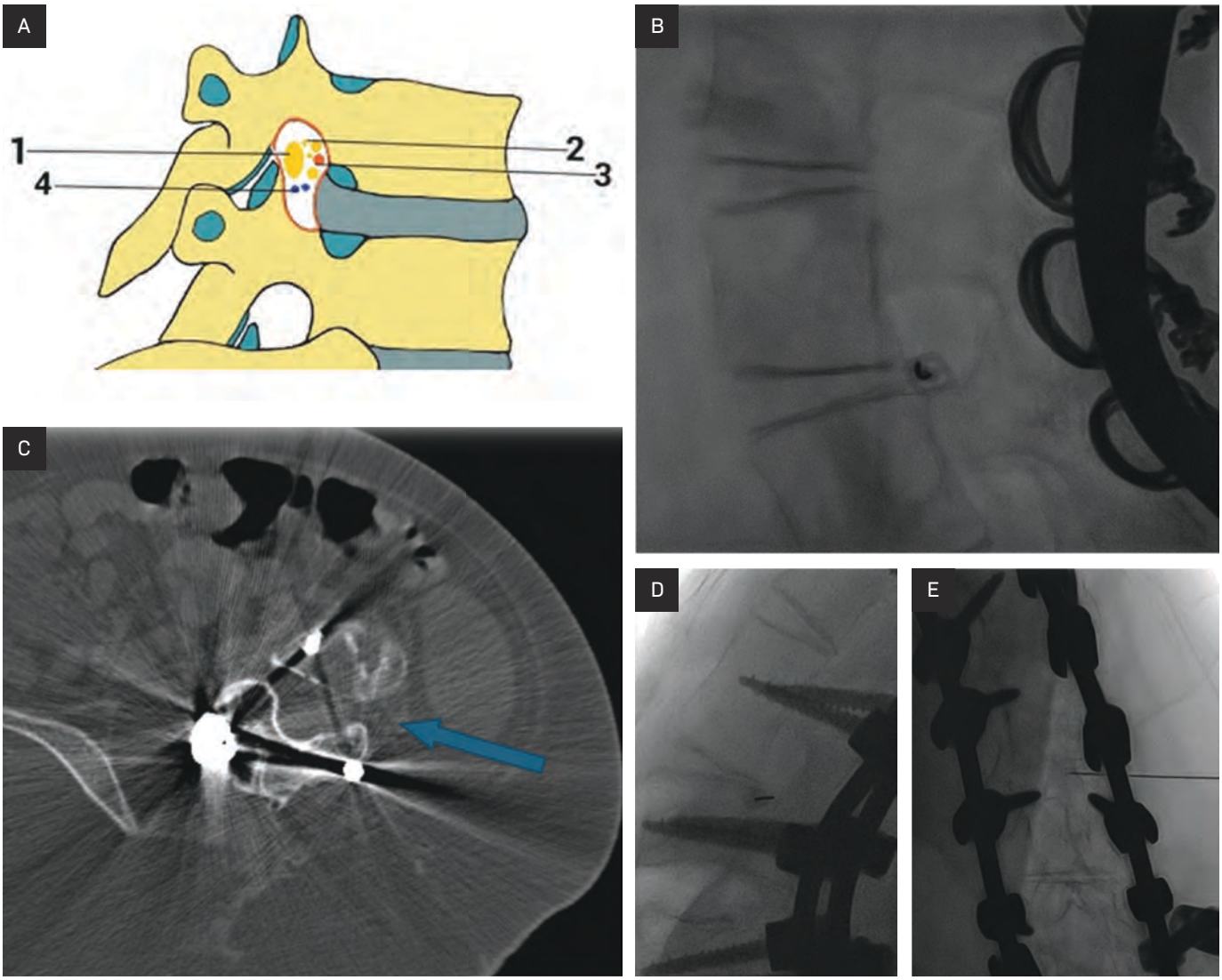

that present with severe hypotonia. Possible conditions include congenital muscular and neuropathic disorders. For SMA types 3 and 4, a limb-girdle muscular dystrophy is the main differential diagnosis.

Discussion

SMA is an inherited, autosomal-recessive neuromuscular disorder most often caused by a homozygous deletion or mutation of the SMN1 gene on chromosome 5q13 with absent exon 7, which results in absent or deficient levels of SMN protein. A second and nearly identical gene, SMN2, produces low levels of functional SMN protein that fails to compensate for the loss of SMN1.[1,2] SMN facilitates the assembly of spliceosomal small nuclear ribonucleoprotein particles, which are thought to function in motor neuron growth and neuromuscular maturation.[3] Over time, SMA results in the degeneration of anterior horn cells in the spinal cord with associated destruction of alpha motor units in lower motor neurons.

SMA presents with varying clinical phenotypes and is classified into 5 main subtypes, based on severity and age of onset. All are characterized by progressive muscle weakness, reduced tone, and atrophy. However, cognition is not affected. Type 0 is congenital SMA, which presents early in neonatal life as severe hypotonia, early respiratory

Figure 3. C1-2 puncture. (A) A fluoroscopic image with the patient in supine position selecting the skin entry site. The needle is over the spinolaminar line just below the skull base. (B) Using intermittant biplane fluoroscopy the needle is guided into the cervical subarachnoid space with the needle tip at midline.

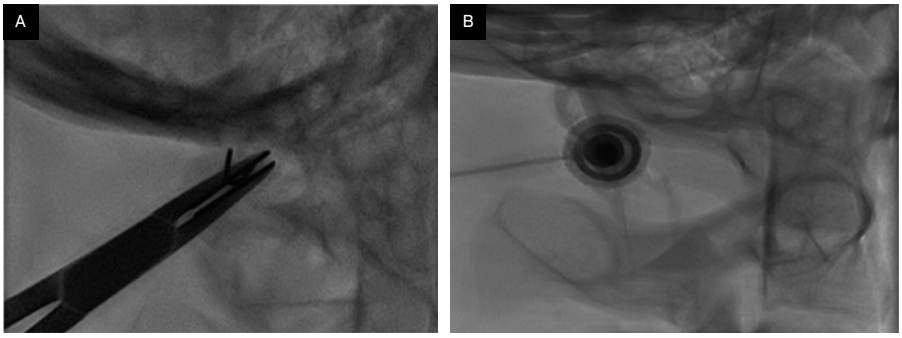

failure, and severe weakness, with death occurring at birth or within the first month of life without treatment. Type 1 is also known as Werdnig-Hoffman disease and presents in the first 6 months of life with limited head control, hypotonia, areflexia, weakness of intercostal muscles, swallowing difficulties, and tongue fasciculations. Type 2, Dubowitz disease, is of intermediate severity, presenting between 6 and 18 months of age. Children with SMA 2 can sit but have hypotonia, areflexia, progressive scoliosis, and restrictive lung disease. Mortality is most commonly due to respiratory compromise, but 70% of patients survive until age 25. Type 3, Kugelberg-Welander disease, is mild SMA presenting after 18 months of age, with progressive proximal weakness in the legs more than the arms. Type 3 patients are ambulatory and typically do not have restrictive lung disease. Additionally, their life expectancy is not affected. Finally, type 4 is adult-onset SMA. It has the mildest phenotype and presents in patients older than 21 years of age, with progressive mild proximal weakness typically not impairing ambulation or affecting life expectancy.[4] With treatment, approximately two-thirds to three-fourths of patients achieve meaningful improvement such as better muscle strength, functional mobility, and breathing.

If clinical history and physical exam findings raise suspicion for SMA, the diagnosis is confirmed by molecular genetic testing to detect homozygous exon 7 deletion in the SMN1 gene, which is 100% specific for the diagnosis of SMA. Around 5% of patients with SMA are compound heterozygotes with a single SMN1 deletion and a frameshift, nonsense, or missense mutation in the other SMN1 copy. SMN2 differs from SMN1 by a single nucleotide, which disrupts a splice enhancer in exon 7, producing an unstable protein that is unable to compensate for the loss of SMN1. However, approximately 10-20% fully functional, full-length transcripts are generated from SMN2. There are 0-8 SMN2 copies in the genome, which is inversely correlated with disease severity. A higher copy number of SMN2 is often able to produce a milder type 2 or 3 phenotype of SMA. In the normal population, the SMN2 copy number varies from 0 to 3 copies, with 15% of normal individuals having no SMN2. An analysis of 625 unrelated Spanish patients with SMA showed that the majority of individuals with type 1 SMA had 1-2 SMN2 copies, most people with type 2 SMA had 3 gene copies, and those with type 3 had 3-4 SMN2 copies.[5] SMN2 copy number detection may be performed to prognose disease severity.[6] Additional tests, including electromyography, muscle biopsy, and creatine kinase, may also support the diagnosis, though these are not first-line tests.

There are no pathognomonic imaging findings diagnostic of SMA. However, over time children may develop scoliosis because of the imbalance between the flexor and extensor muscles of the trunk, typically leading to a C-shaped, neuromuscular curvature of the spine (Figure 1). If the degree of scoliosis is severe or progressive, instrumentation and spinal fusion are often necessary, as in this patient. The severity of the curvature, the vertebral rotation, and spinal fixation may make traditional IT access for nusinersen administration challenging.

Therapeutic approaches are multifold, including splicing modification of SMN2 via antisense oligonucleotides (ASO), small molecules that modulate SMN2 gene splicing, and SMN1 gene replacement therapy. Nusinersen (Spinraza, Biogen), the first molecular drug to treat SMA, is an intrathecally administered ASO that promotes the inclusion of exon 7 in mRNA transcripts of SMN2, resulting in translation of a higher level of fully functional SMN protein in liver, kidney, skeletal muscle, and central nervous system tissues. Patients with SMA have experienced significant improvement in motor function and extensions in life expectancy after receiving nusinersen.[7] IT administration of nusinersen introduces unique challenges based on whether patients have simple or complex spinal anatomy (neuromuscular scoliosis, spinal fusion, or instrumentation) (Figure 1). There are several approaches that can be used to facilitate drug injection into the subarachnoid space. In children with uncomplicated spines, a midline lumbar puncture is performed. In those with complex spines, a transforaminal (Figure 2) or C1-2 approach may be performed (Figure 3). The authors prefer the transforaminal approach as it is safer and technically easier.[8,9] Multiple reviews showed that complex SMA anatomy usually requires preprocedural imaging for route planning and intraprocedural guidance to access the subarachnoid space via the transforaminal approach.[8,9]

A newer, orally administered small molecule has also been developed to treat SMA, called risdiplam (Evrysdi, Genentech). This drug modulates SMN2 gene splicing by binding 2 pre-mRNA

https://doi.org/10.37549/JPCR-26-0082

splice sites in exon 7, increasing the levels of full-length SMN mRNA and protein. It has enhanced specificity toward exon 7 splicing relative to other SMN2 splicing modifiers, decreasing the probability of off-target effects. Risdiplam crosses the blood-brain barrier, achieving systemic distribution with suitable half-life and predictable pharmacokinetics.[10] Onasemnogene abeparvovec (Zolgensma, Novartis) is SMN1 gene replacement therapy, which uses a nonreplicating adeno-associated virus capsid carrying SMN1 complementary recombinant DNA to efficiently deliver wild-type SMN1 gene to motor neuron cells. A one-time intravenous injection leads to systemic expression of the SMN protein in SMA mice.[11]

Additionally, there are investigations relating to muscle-enhancing therapies that target SMN-independent factors and may provide additional therapeutic benefit in combination with SMN-targeting treatments. Reldesemtiv (an investigational drug) is a small-molecule troponin activator in fast skeletal muscles, reinforcing contraction and promoting muscle response to nervous stimulus.[11] SRK-015 is a monoclonal antibody that selectively inhibits myostatin, promoting muscle cell growth, differentiation, and force in SMA mice.[11] Additional research on SMN-independent factors is ongoing, and potential therapeutic targets include autophagosomes, which are increased in SMA motor neurons and may be decreased with IM injections of neurotrophic factor tetanus toxin heavy chain or intracerebroventricular administration of 3-MA.[11] Additionally, SMA mice have been shown to have a deficiency in agrin expression, which is a synaptic organizer functioning in the efficiency of neuromuscular transmission, an effect that may be relieved with the administration of C-terminal fragment of agrin.[12]

Gene therapy has transformed types 0 and 1 SMA from a fatal disease into a treatable condition or decreases the severity of the disease. It is common for patients to show improved motor function and survival rates.

Conclusion

SMA is an inherited neuromuscular disorder characterized by progressive muscle weakness. It has varying clinical severity ranging from mild proximal muscle weakness to death from restrictive lung disease. The diagnosis is confirmed by genetic testing. Treatment includes SMN2 splicing modulator nusinersen, which may be challenging to administer intrathecally as patients develop varying degrees of scoliosis over time, making midline or paramedian lumbar punctures difficult. Patients with complex spinal anatomy may benefit from preprocedural and intraprocedural imaging to allow for a transforaminal approach for the IT administration of nusinersen. Additional SMA treatments include risdiplam, a newer, oral splicing modulator, or SMN1 gene replacement therapy with Zolgensma.

References

1) Prior TW, Leach ME. Spinal muscular atrophy. In: Finanger E, Adam MP, Ardinger HH, Pagon RA, et al, eds. *GeneReviews®* [Internet]. University of Washington, Seattle. 2000.

2) Kolb SJ, Kissel JT. Spinal muscular atrophy. *Neurol Clin*. 2015;33(4):831-846. doi:10.1016/j.ncl.2015.07.004

3) Fan L, Simard LR. Survival Motor Neuron (SMN) protein: role in neurite outgrowth and neuromuscular maturation during neuronal differentiation and development. *Hum Mol Genet*. 2002;11(14):1605-1614. doi:10.1093/hmg/11.14.1605

4) Burr P, Reddivari AKR. Spinal muscle atrophy. In: *StatPearls* [Internet]. StatPearls Publishing. 2021.

5) Calucho M, Bernal S, Alías L, et al. Correlation between SMA type and SMN2 copy number revisited: an analysis of 625 unrelated Spanish patients and a compilation of 2834 reported cases. *Neuromuscul Disord*. 2018;28(3):208-215. doi:10.1016/j.nmd.2018.01.003

6) Rouzier C, Chaussenot A, Paquis-Flucklinger V. Molecular diagnosis and genetic counseling for Spinal Muscular Atrophy (SMA). *Arch Pediatr*. 2020;27(7s):7S9-7S14. doi:10.1016/S0929-693X(20)30270-0

7) Paton DM. Nusinersen: antisense oligonucleotide to increase SMN protein production in spinal muscular atrophy. *Drugs Today (Barc)*. 2017;53(6):327-337. doi:10.1358/dot.2017.53.6.2652413

8) Mousa MA, Aria DJ, Schaefer CM, et al. A comprehensive institutional overview of intrathecal nusinersen injections for spinal muscular atrophy. *Pediatr Radiol*. 2018;48(12):1797-1805. doi:10.1007/s00247-018-4206-9

9) Towbin R, Schaefer C, Kaye R, Abruzzo T, Aria DJ. The complex spine in children with spinal muscular atrophy: the transforaminal approach-A transformative technique. *AJNR Am J Neuroradiol*. 2019;40(8):1422-1426. doi:10.3174/ajnr.A6131

10) Ratni H, Ebeling M, Baird J, et al. Discov-ery of risdiplam, a selective Survival of Motor Neuron-2 (SMN2) gene splicing modifier for the treatment of Spinal Muscular Atrophy (SMA). *J Med Chem*. 2018;61(15):6501-6517. doi:10.1021/acs. jmedchem.8b00741

11) Messina S, Sframeli M. New treatments in spinal muscular atrophy: positive results and new challenges. J Clin Med. 2020;9(7):2222. doi:10.3390/jcm9072222

12) Boido M, De Amicis E, Valsecchi V, et al. Increasing agrin function antagonizes muscle atrophy and motor impairment in spinal muscular atrophy. Front Cell Neurosci. 2018;12:17. doi:10. 3389/fncel.2018.00017

Clubfoot

Hunter Glover, MS; Richard B. Towbin, MD; Carrie M. Schaefer, MD; Alexander J. Towbin, MD

Abstract

Talipes equinovarus, or clubfoot, represents a spectrum of foot deformities characterized by hindfoot equinus and varus with forefoot adduction and supination. Most cases reflect congenital structural malalignment and are classified as idiopathic, syndromic, or neurogenic, while postural deformities are flexible and nonstructural. Prenatal diagnosis is typically established with US, and postnatal evaluation relies on clinical examination with selective use of radiographs. Weight-bearing or simulated weight-bearing anteroposterior and lateral radiographs allow measurement of the talocalcaneal and tibiocalcaneal angles, which aid in assessing severity and monitoring correction. The Ponseti method of serial casting remains the gold standard treatment, although relapse may occur and can be identified clinically or radiographically.

Keywords: mulsculoskeletal, foot, congenital

Case Summary

A young child with a known diagnosis of clubfoot presented to the orthopedic clinic for corrective management.

Imaging Findings

Anteroposterior and lateral simulated weight-bearing radiographs of the foot demonstrate findings consistent with clubfoot deformity. On the anteroposterior view, the talus and calcaneus are nearly parallel, reflecting hindfoot varus. On the lateral view, the talocalcaneal angle measures 16°, decreased relative to the normal range of 25-55°. The tibiocalcaneal angle measures 117° increased relative to the normal range of 25-60° in maximum dorsiflexion. These findings are consistent with hindfoot equinus and varus deformity (Figure 1).

Diagnosis

Clubfoot

Discussion

Talipes equinovarus, commonly referred to as clubfoot, describes a spectrum of foot deformities characterized by hindfoot equinus and varus with forefoot adduction and supination. The condition most commonly represents a congenital structural malalignment of the talus and adjacent hindfoot structures, with associated medial and posterior soft-tissue contractures, including shortening of the Achilles tendon and medial ligaments. Clubfoot is one of the most common congenital lower extremity deformities, occurring in approximately 0.5-3 per 1000 live births worldwide, with higher rates reported in certain populations and a male predominance of approximately 2:1.[1-3]

Clubfoot is broadly classified into 4 categories: postural, idiopathic, syndromic, and neurogenic.[4] Postural clubfoot accounts for approximately 10% of cases and results from intrauterine positioning forces. These deformities are flexible and typically respond to stretching and casting alone.[1,2] The remaining categories represent structural forms in which the deformity is rigid and not correctable with passive manipulation. Idiopathic clubfoot is the most common form and occurs in the absence of associated anomalies. Syndromic clubfoot is associated with chromosomal abnormalities, genetic syndromes, skeletal dysplasias, and connective tissue disorders. Common associations include arthrogryposis, Down syndrome, diastrophic dysplasia, and TARP (Talipes equinovarus, Atrial septal sefect, Robin sequence, Persistent left superior vena cava) syndrome.[1,2,5] Neurogenic clubfoot results from disruption of the neuromuscular unit and may be seen in conditions such as myelomeningocele.[1,2,5]

Prenatal diagnosis of clubfoot is most commonly established during the first or second trimester using US. Reported

Affiliations: UNTHSC Texas College of Osteopathic Medicine, Fort Worth, Texas (Glover); Department of Radiology, Phoenix Children's Hospital, Phoenix, Arizona (RB Towbin, Schaefer); Department of Radiology, Cincinnati Children's Hospital, University of Cincinnati College of Medicine, Cincinnati, Ohio (AJ Towbin).
Disclosures: The authors have no conflicts of interest to disclose. None of the authors received outside funding for the production of this original manuscript and no part of this article has been previously published elsewhere.

https://doi.org/10.37549/JPCR-26-0083

Figure 1. (A) Anteroposterior simulated weight-bearing radiograph of the foot demonstrating parallel alignment of the talus and calcaneus, consistent with hindfoot varus and forefoot adduction. (B) Lateral simulated weight-bearing radiograph demonstrating hindfoot equinus with a decreased lateral talocalcaneal angle and an increased tibiocalcaneal angle. (C) Anteroposterior radiograph demonstrating measurement of the talocalcaneal angle, formed by lines drawn through the longitudinal axes of the talus and calcaneus. (D) Lateral radiograph demonstrating measurement of the lateral talocalcaneal angle using the longitudinal axes of the talus and calcaneus. (E) Lateral radiograph demonstrating measurement of the tibiocalcaneal angle, formed by the longitudinal axes of the tibia and calcaneus.

diagnostic accuracy is approximately 86%.[1,6] Fetal MRI may be considered when additional skeletal abnormalities are suspected on US. Following delivery, physical examination confirms or excludes the diagnosis. Postural deformities related to intrauterine constraint should be considered in the differential diagnosis, as these may mimic structural clubfoot on prenatal imaging but are typically reducible on postnatal examination.[1,2]

Radiographs may be used to assess deformity severity and to evaluate correction during and after intervention. Standard imaging includes anteroposterior and lateral weight-bearing or simulated weight-bearing views. On the anteroposterior view, the talocalcaneal angle is formed by the intersection of the longitudinal axes of the talus and calcaneus. On the lateral view, the talocalcaneal angle is measured using the same axes in the sagittal plane. The tibiocalcaneal angle, measured on the lateral view, is formed by the intersection of the longitudinal axis of the tibia and the longitudinal axis of the calcaneus (Figure 1).

Reported normal ranges are 15-55° for the anteroposterior talocalcaneal angle, 25-55° for the lateral talocalcaneal angle, and 25-60° for the tibiocalcaneal angle in maximum dorsiflexion.[7,8] In clubfoot, the lateral talocalcaneal angle is typically decreased and the tibiocalcaneal angle increased, reflecting hindfoot varus and equinus.

The gold standard treatment for clubfoot is the Ponseti method of serial casting, with Achilles tenotomy required in up to 90% of cases.[2,3,5] Early intervention prior to ambulation and continued bracing through early childhood are associated with improved outcomes. Treatment begins with correction of the cavus deformity by supinating the forefoot and applying pressure beneath the first metatarsal head. Hindfoot varus, forefoot adduction, and hindfoot equinus are then sequentially corrected over several casting sessions. Following tenotomy and application of a final long-leg cast, patients are transitioned to a foot abduction brace to reduce the risk of relapse.

Relapse is defined as the recurrence of any component of the deformity after treatment. It may be identified clinically or radiographically, with lateral radiographs helping assess persistent equinus or varus deformity.[5-7] Although initial correction rates approach 92% in patients treated with the Ponseti method, relapse occurs in approximately one-third of patients, with reported long-term recurrence rates ranging from 3% to 62.5%.[2,5,8] Greater initial deformity

severity and poor brace compliance are associated with increased relapse risk. Recurrent or residual deformity may result in overcorrection, undercorrection, bunion formation, ankle impingement, and degenerative changes, sometimes requiring additional intervention to preserve function and alleviate pain.[9]

Conclusion

Talipes equinovarus, or clubfoot, represents a spectrum of foot deformities characterized by hindfoot equinus and varus with forefoot adduction and supination. Most cases reflect congenital structural malalignment and are classified as idiopathic, syndromic, or neurogenic, while postural deformities are flexible and nonstructural. Prenatal diagnosis is typically established with US, and postnatal evaluation relies on clinical examination with selective use of radiographs. Weight-bearing or simulated weight-bearing anteroposterior and lateral radiographs allow measurement of the talocalcaneal and tibiocalcaneal angles, which aid in assessing severity and monitoring correction. The Ponseti method of serial casting remains the gold standard treatment, although relapse may occur and can be identified clinically or radiographically.

References

1) Martin S. Clubfoot (talipes equinovarus). In: *Obstetric imaging: fetal diagnosis and care*. 2nd ed. Elsevier. 2018. https://www-clinicalkey-com.proxy.unthsc.edu/#!/content/book/3-s2.0-B9780323445481000644

2) Rieger MA, Dobbs MB. Clubfoot. *Clin Podiatr Med Surg*. 2022;39(1):1-14. doi:10.1016/j.cpm.2021.08.006

3) Williams ML, Dobbs MB. Clubfoot. *Clin Podiatr Med Surg*. 2024;41(1):17-25. doi:10.1016/j.cpm.2023.06.009

4) Green A. The pediatric foot and ankle. *Pediatr Clin North Am*. 2020;67(1):169-183. doi:10.1016/j.pcl.2019.09.007

5) Dobbs MB, Gurnett CA. Update on clubfoot: etiology and treatment. *Clin Orthop Relat Res*. 2009;467(5):1146-1153. doi:10.1007/s11999-009-0734-9

6) Fantasia I, Dibello D, Di Carlo V, et al. Prenatal diagnosis of isolated clubfoot: diagnostic accuracy and long-term postnatal outcomes. *Eur J Obstet Gynecol Reprod Biol*. 2021;264:60-64. doi:10.1016/j.ejogrb.2021.07.009

7) Moerman S, Zijlstra-Koenrades N, Reijman M, et al. The predictive value of radiographs and the pirani score for later additional surgery in ponseti-treated idiopathic clubfeet, an observational cohort study. *Children*. 2022;9(6):865. doi:10.3390/children9060865

8) Zhang G, Zhang Y, Li M. A modified PONSETI method for the treatment of rigid idiopathic congenital clubfoot. *J Foot Ankle Surg*. 2019;58(6):1192-1196. doi:10.1053/j.jfas.2019.04.003

9) Johnson JE, Fortney TA, Luk PC, et al. Late effects of clubfoot deformity in adolescent and young adult patients whose initial treatment was an extensive soft-tissue release: topic review and clinical case series. *J Am Acad Orthop Surg Glob Res Rev*. 2020;4(5):e19.00126. doi:10.5435/JAAOSGlobal-D-19-00126

Neutropenic Colitis

Nicholas T. Weigle, BS; Richard B. Towbin, MD; Carrie M. Schaefer, MD; Alexander J. Towbin, MD

Abstract

Neutropenic colitis is an uncommon but life-threatening complication that occurs in patients receiving cytotoxic chemotherapy, particularly for hematologic malignancies. Early recognition of symptoms, such as abdominal pain, fever, and diarrhea, is critical. Prompt diagnostic imaging plays a pivotal role in confirming the diagnosis and excluding other potential causes of abdominal symptoms. Early detection enables the timely initiation of appropriate treatment, including broad-spectrum antibiotics and supportive care, which is essential to reduce morbidity and mortality associated with this condition. It is identified clinically or radiographically.

Keywords: gastrointestinal, intestines, oncology, immune suppression

Case Summary

An infant with B-cell acute lymphoblastic leukemia treated with chemotherapy was neutropenic. The patient developed worsening tachypnea, abdominal distention, abdominal wall erythema and edema, and lactic acidosis.

Imaging Findings

Abdominal CT (Figure 1) showed dilated bowel loops with diffuse colonic wall thickening, wall edema, and moderate ascites.

Diagnosis

Neutropenic colitis

The clinical differential diagnosis includes infectious colitis, ischemic colitis, appendicitis, inflammatory bowel disease, graft-versus-host disease, and cytomegalovirus colitis.

Discussion

Neutropenic colitis, also known as typhlitis, is a life-threatening inflammatory condition of the bowel, typically involving the cecum, ascending colon, and terminal ileum in immunocompromised patients.[1] The condition is characterized by mucosal injury, bowel wall edema, and inflammation, compounded by profound neutropenia that compromises the body's ability to mount an effective immune response.

It most commonly occurs in patients undergoing cytotoxic chemotherapy for hematologic malignancies, particularly acute leukemia.[2,3] However, it has also been reported in patients treated for lymphoma, multiple myeloma, and solid tumors, as well as in individuals with nonmalignant causes of neutropenia, including aplastic anemia, cyclic neutropenia, agranulocytosis, Felty syndrome, thalassemia minor, systemic lupus erythematosus, and HIV infection.[3,4] In hospitalized patients with hematologic malignancies, the reported prevalence of neutropenic colitis is approximately 2.6%.[4]

Neutropenic colitis is thought to result from chemotherapy-induced mucosal injury combined with profound neutropenia, which predisposes patients to bacterial invasion of the bowel wall.[2,5] Symptoms typically develop within 2 weeks after completing chemotherapy and include abdominal pain, fever, and diarrhea.[2,5] When neutropenia is identified during laboratory monitoring and clinical symptoms are present, diagnostic imaging should be performed to evaluate for neutropenic colitis.

The diagnostic criteria for neutropenic colitis include the presence of neutropenia (absolute neutrophil count $< 500 \times 10^6$ cells/L), bowel wall thickening greater than 4 mm on imaging, and exclusion of alternative diagnoses.[3] CT and/or abdominal US is the initial imaging of choice for diagnosis, as it not only confirms bowel wall thickening but also evaluates for other causes of abdominal pain, such as appendicitis or gastroenteritis.[4,6] In addition to wall thickening, imaging findings may include cecal or colonic dilation, an inflammatory mass, pericolic inflammation/abscess, pneumatosis intestinalis, or perforation.[2,6]

Abdominal radiographs in neutropenic colitis may demonstrate a dilated, atonic cecum and ascending colon filled with

Affiliations: School of Medicine, Wayne State University, Detroit, Michigan (Weigle); Department of Radiology, Phoenix Children's Hospital, Phoenix, Arizona (RB Towbin, Schaefer); Department of Radiology, Cincinnati Children's Hospital, University of Cincinnati College of Medicine, Cincinnati, Ohio (AJ Towbin).
Disclosures: The authors have no conflicts of interest to disclose. None of the authors received outside funding for the production of this original manuscript and no part of this article has been previously published elsewhere.

https://doi.org/10.37549/JPCR-26-0084

Figure 1. (A) Axial and (B, C) sequential coronal images from an abdominal CT showing massive bowel wall thickening extending from the terminal ileum (arrow) through the descending colon (arrowhead) and rectum (not shown). Moderate ascites was also present.

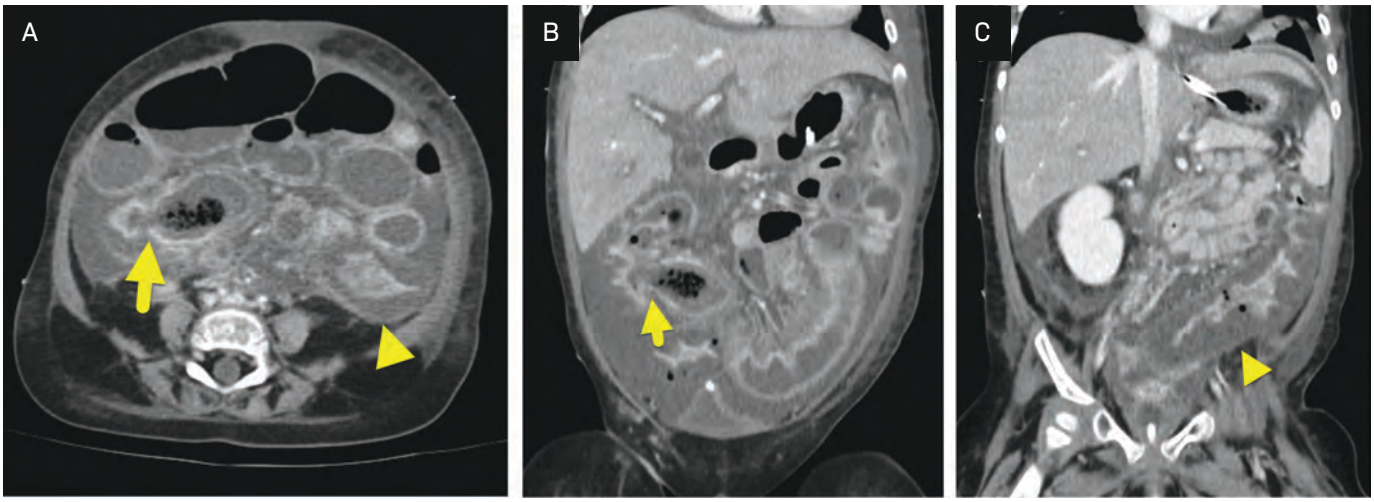

liquid or gas.[6] US findings supportive of the diagnosis include bowel wall thickening, pericolic fluid collections, increased echogenicity of the bowel wall or mesenteric fat, the presence of 3 or more enlarged mesenteric lymph nodes greater than 5 mm in short axis, hyperemia on Doppler or contrast-enhanced US, and abnormal peristalsis.[6,7] US is commonly utilized in pediatric populations and can be as accurate as CT in detecting bowel wall thickening and increased vascularity of the bowel wall and mesentery, thereby aiding in the diagnosis of neutropenic colitis.[6]

Major complications and causes of mortality in neutropenic colitis include necrotizing bowel perforation, gastrointestinal bleeding, and sepsis.[5,8] Even with appropriate management, mortality rates range from 23% to 31%.[8] Prompt imaging is critical at the onset of symptoms to reduce morbidity and mortality. Early detection is possible through careful adherence to chemotherapy surveillance and laboratory monitoring protocols.

Treatment for neutropenic colitis includes broad-spectrum antibiotics to address potential pathogens.[2,8] Supportive care is equally important, with interventions such as fluid resuscitation, correction of electrolyte imbalances, and bowel rest to protect and promote healing of the intestinal mucosa.[2,8] These measures aim to stabilize the patient and allow for mucosal recovery while minimizing the risk of further complications.

Conclusion

Neutropenic colitis is an uncommon but life-threatening complication that occurs in patients receiving cytotoxic chemotherapy, particularly for hematologic malignancies. Early recognition of symptoms, such as abdominal pain, fever, and diarrhea, is critical. Prompt diagnostic imaging plays a pivotal role in confirming the diagnosis and excluding other potential causes of abdominal symptoms. Early detection enables the timely initiation of appropriate treatment, including broad-spectrum antibiotics and supportive care, which is essential to reduce morbidity and mortality associated with this condition.

References

1) Bertozzi G, Maiese A, Passaro G, et al. Neutropenic enterocolitis and sepsis: towards the definition of a pathologic profile. *Medicina (Kaunas)*. 2021;57(6):638. doi:10.3390/medicina57060638

2) Rodrigues FG, Dasilva G, Wexner SD. Neutropenic enterocolitis. *World J Gastroenterol*. 2017;23(1):42-47. doi:10.3748/wjg.v23.i1.42

3) Nesher L, Rolston KVI. Neutropenic enterocolitis, a growing concern in the era of widespread use of aggressive chemotherapy. *Clin Infect Dis*. 2013;56(5):711-717. doi:10.1093/cid/cis998

4) McCarville MB, Adelman CS, Li C, et al. Typhlitis in childhood cancer. *Cancer*. 2005;104(2):380-387. doi:10.1002/cncr.21134

5) Benedetti E, Traverso G, Pucci G, et al. Impact of different chemotherapy regimens on intestinal mucosal injury assessed with bedside ultrasound: a study in 213 AML patients. *Front Oncol*. 2023;13:1272072. doi:10.3389/fonc.2023.1272072

6) Tamburrini S, Setola FR, Belfiore MP, et al. Ultrasound diagnosis of typhlitis. *J Ultrasound*. 2019;22(1):103-106. doi:10.1007/s40477-018-0333-2

7) Hwang JY. Emergency ultrasonography of the gastrointestinal tract of children. *Ultrasonography*. 2017;36(3):204-221. doi:10.14366/usg.16052

8) Machado NO. Neutropenic enterocolitis: a continuing medical and surgical challenge. *N Am J Med Sci*. 2010;2(7):293-300.

Slipped Capital Femoral Epiphysis

Kaab Husain, BS; Richard B. Towbin, MD; Carrie M. Schaefer, MD; Alexander J. Towbin, MD

Abstract

Slipped capital femoral epiphysis (SCFE) typically affects adolescents aged 8-15 and has a multifactorial etiology, with risk factors related to race, obesity, and seasonal variation. Patients typically present with a limp and pain localized to the groin, lateral or posterior hip, thigh, or ipsilateral knee. Radiographic findings include physeal widening, irregularity, and decreased epiphyseal height on anteroposterior views. Prompt recognition and surgical management are essential to prevent further slippage, preserve femoral head vascularity, and restore mobility.

Keywords: musculoskeletal, hips, trauma

Case Summary

An adolescent male was referred to an ambulatory orthopedic surgery clinic with a 1-week history of a painless limp.

Imaging Findings

Radiograph of the hips (Figure 1) showed mild widening of the left proximal femoral physis and medial displacement of the left femoral head.

Diagnosis

Slipped capital femoral epiphysis (SCFE).

The differential diagnosis for SCFE includes idiopathic avascular necrosis of the femoral head (Legg-Calvé-Perthes disease), femoral neck stress fracture, adductor muscle strain, septic arthritis, or osteomyelitis.

Figure 1. (A) Anteroposterior and (B) frog-leg lateral views of the pelvis. The physis of the left proximal femur (arrow) is lucent, widened, and irregular compared to the contralateral side. The left femoral head is displaced medially in relation to the femoral neck. This is more apparent on the frog-leg view.

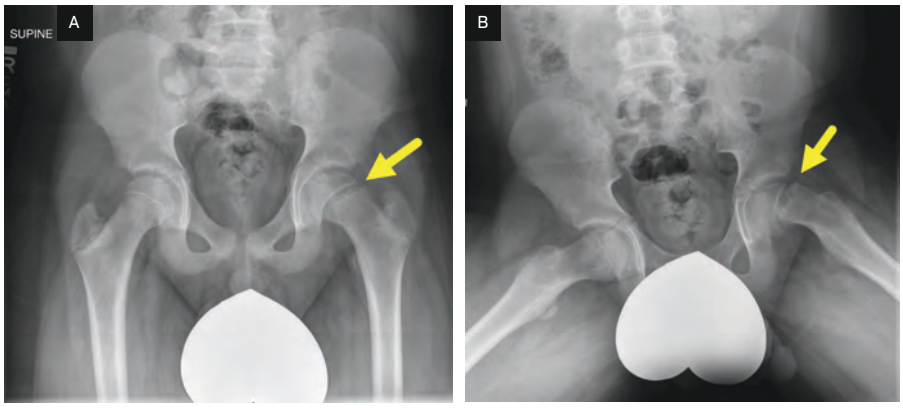

Discussion

SCFE is the most common hip disorder in adolescents. It typically affects children between 8 and 15 years of age, with a US incidence of 10.8 cases per 100,000.[1,2] Bilateral involvement occurs in 18-50% of patients, with 50-60% of those being simultaneous.[3] In children who develop sequential bilateral SCFE, 80-90% of the contralateral slips occur within 18 months of the initial diagnosis.[3]

SCFE remains a diagnostic challenge due to its gradual onset and nonspecific symptoms, which often mimic other musculoskeletal conditions. Children typically present with chronic hip, groin, or thigh pain that may radiate to the ipsilateral knee. The pain usually worsens with activity and improves with rest. Additional clinical signs include limping, stiffness, and a reduced

Affiliations: School of Medicine, Wayne State University, Detroit, Michigan (Husain); Department of Radiology, Phoenix Children's Hospital, Phoenix, Arizona (RB Towbin, Schaefer); Department of Radiology, Cincinnati Children's Hospital, University of Cincinnati College of Medicine, Cincinnati, Ohio (AJ Towbin).
Disclosures: The authors have no conflicts of interest to disclose. None of the authors received outside funding for the production of this original manuscript and no part of this article has been previously published elsewhere.

https://doi.org/10.37549/JPCR-26-0085

Figure 2. Frog-leg lateral view of the pelvis showing how to calculate the Southwick angle. The first line (1) is drawn connecting the epiphyseal margins, a second line (2) is drawn perpendicular to the first, and, finally, a third line (3) is drawn from the intersection of the perpendicular lines along the axis of the femoral diaphysis. This value is then compared with the corresponding angle on the contralateral side, and the difference yields the final Southwick angle.

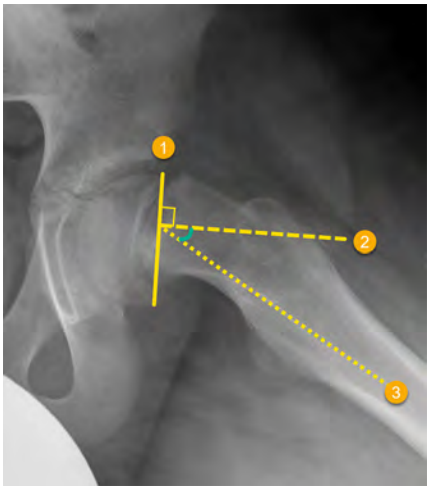

range of hip motion.[4,5] A history of trauma is uncommon. SCFE occurs when the capital femoral epiphysis "slips," displacing posteriorly and inferiorly through the weakened, fractured growth plate. While the condition is often idiopathic, contributing factors include mechanical shear stress across the physis and conditions that reduce physeal integrity or increase axial load, such as obesity and endocrine disorders.[4]

The risk of SCFE is influenced by several demographic factors. Males are significantly more likely to develop SCFE than females (OR 1.73; 95% CI, 1.51-1.97).[6] Seasonal variation has been observed in North America, with higher incidence rates during the summer and fall, likely due to increased activity.[6] SCFE is also more common in the northeastern United States and among African American children. Prompt and accurate diagnosis is critical, as delayed treatment can lead to serious complications, including avascular necrosis (AVN) and early-onset degenerative hip arthritis.

Due to its nonspecific presentation, SCFE can be mistaken for other hip pathologies, including femoroacetabular impingement, Legg-Calvé-Perthes disease, and hip dysplasia. Given the risk of serious complications if left untreated, radiographs should be obtained in any child with SCFE included in the differential diagnosis.

SCFE is classified by clinical stability and severity, with newer classification systems emphasizing physeal stability due to its strong predictive value for complications such as AVN. Clinically, SCFE is divided into stable and unstable forms. In stable SCFE, the child can bear weight—with or without crutches—indicating preserved blood supply to the femoral head and a very low risk of AVN, often approaching 0%.[7] These patients generally have favorable outcomes with appropriate treatment. In contrast, unstable SCFE is characterized by an inability to ambulate due to pain and physeal instability. This form is associated with a significantly higher risk of osteonecrosis, with reported rates ranging from 20% to 50%, and requires urgent surgical intervention to stabilize the physis and protect vascular integrity.[7]

Plain-film radiography remains the gold standard for diagnosing SCFE. Anteroposterior (AP) pelvis and frog-leg lateral views of both hips should be obtained in patients with symptoms of stable SCFE. In patients with suspected unstable SCFE, the frog-leg view should be avoided and replaced by a cross-table lateral view to minimize displacement risk. Key radiographic features of SCFE include physeal widening or irregularity compared with the contralateral side, decreased epiphyseal height on AP views, and loss of the anterior concavity of the femoral neck on lateral views. The "metaphyseal blanch sign"—a crescent-shaped area of increased density seen on AP radiographs—is caused by superimposition of the posteriorly and inferiorly displaced epiphysis over the metaphysis. Chronic SCFE may demonstrate metaphyseal cystic changes, remodeling, or a periosteal reaction. In severe or longstanding cases, chondrolysis and subchondral bone changes involving both the femur and acetabulum may also be observed.[8]

SCFE severity can be assessed radiographically using 2 primary methods: the percentage of epiphyseal displacement and the Southwick angle. The first method estimates the degree of slippage relative to the metaphyseal width: mild (< 1/3), moderate (1/3-1/2), and severe (>1/2). A more precise and prognostically useful measurement is the Southwick angle, typically assessed on frog-leg lateral radiographs. This angle is calculated in several steps (Figure 2). First, a line is drawn connecting the margins of the capital femoral epiphysis, a second line is drawn perpendicular to the first, and a third line is drawn along the axis of the femoral diaphysis. The angle between the second and third lines is measured. This value is then compared with the corresponding angle on the contralateral side, and the difference yields the final Southwick angle. Mild SCFE is defined as an angle less than 30°, moderate as 30-50°, and severe as greater than 50°.[9] Increasing angular deformity is associated with a higher risk of early-onset degenerative hip disease.

In the early stages of SCFE, radiographs and CT scans may fail to detect subtle or impending slips. MRI is more sensitive than radiographs for detecting early or pre-slip changes. Early MRI findings include physeal widening, marrow edema (best seen on T1-weighted images), joint effusion (best appreciated on T2-weighted images), and early signs of slippage.[10] Despite its higher sensitivity, MRI is typically reserved for cases in which SCFE is suspected but not confirmed on radiographs, or when further evaluation of complications is needed after diagnosis.

The primary goal of SCFE management is to prevent further slippage of the femoral head and to reduce the risk of complications such as AVN, chondrolysis, and early osteoarthritis. Chondrolysis—characterized by progressive cartilage loss and joint stiffness—affects 1-7% of

patients.[7] Residual deformities may lead to early osteoarthritis in 25-50% of cases.[7]

In situ screw fixation is the standard treatment for stable SCFE and serves to prevent further slippage. In more severe or unstable cases, the modified Dunn procedure aims to correct proximal femoral deformity, stabilize the epiphysis, and preserve the femoral head's vascular supply, thereby reducing the risk of AVN. When indicated, capsulotomy may be performed to reduce intracapsular pressure and mitigate ischemic injury in patients with unstable SCFE.[11] Despite these interventions, treatment remains technically complex, and careful surgical planning is essential to achieve optimal outcomes.

Conclusion

SCFE typically affects adolescents aged 8-15 and has a multifactorial etiology with risk factors related to race, obesity, and seasonal variation. Patients typically present with a limp and pain localized to the groin, lateral or posterior hip, thigh, or ipsilateral knee. Radiographic findings include physeal widening, irregularity, and decreased epiphyseal height on AP views. Prompt recognition and surgical management are essential to prevent further slippage, preserve femoral head vascularity, and restore mobility.

References

1) Johns K, Mabrouk A, Tavarez MM. Slipped capital femoral epiphysis. In: *StatPearls* [Internet]. StatPearls Publishing. 2023. https://www.ncbi.nlm.nih.gov/books/NBK538302/

2) Lehmann CL, Arons RR, Loder RT, Vitale MG. The epidemiology of slipped capital femoral epiphysis: an update. *J Pediatr Orthop*. 2006;26(3):286-290. doi:10.1097/01.bpo.0000217718.10728.70

3) Loder RT. The demographics of slipped capital femoral epiphysis an international multicenter study. *Clin Orthop Relat Res*. 1996;322(322):8-27. doi:10.1097/00003086-199601000-00003

4) Novais EN, Millis MB. Slipped capital femoral epiphysis: prevalence, pathogenesis, and natural history. *Clin Orthop Relat Res*. 2012;470(12):3432-3438. doi:10.1007/s11999-012-2452-y

5) Uvodich M, Schwend R, Stevanovic O, et al. Patterns of pain in adolescents with slipped capital femoral epiphysis. *J Pediatr*. 2019;206:184-189. doi:10.1016/j.jpeds.2018.10.050

6) Miles DT, Wilson AW, Scull MS, Moses W, Quigley RS. A new look on the epidemiology of slipped capital femoral epiphysis: a topic revisited. *J Pediatr Soc North Am*. 2023;5(4):705. doi:10.55275/JPOSNA-2023-705

7) Peck DM, Voss LM, Voss TT. Slipped capital femoral epiphysis: diagnosis and management. *Am Fam Physician*. 2017;95(12):779-784.

8) Hesper T, Zilkens C, Bittersohl B, Krauspe R. Imaging modalities in patients with slipped capital femoral epiphysis. *J Child Orthop*. 2017;11(2):99-106. doi:10.1302/1863-2548-11-160276

9) Boyer DW, Mickelson MR, Ponseti IV. Slipped capital femoral epiphysis. long-term follow-up study of one hundred and twenty-one patients. *J Bone Joint Surg*. 1981;63(1):85-95. doi:10.2106/00004623-198163010-00011

10) Balch Samora J, Adler B, Druhan S, et al. MRI in idiopathic, stable, slipped capital femoral epiphysis: evaluation of contralateral pre-slip. *J Child Orthop*. 2018;12(5):454-460. doi:10.1302/1863-2548.12.170204

11) Aprato A, Conti A, Bertolo F, Massè A. Slipped capital femoral epiphysis: current management strategies. *Orthop Res Rev*. 2019;11:47-54. doi:10.2147/ORR.S166735

Pectus Excavatum

Dorina V. Pinkhasova, BS; Richard B. Towbin, MD; Carrie M. Schaefer, MD; Cara E. Morin, MD; Alexander J. Towbin, MD

Abstract

Pectus excavatum, commonly known as sunken or funnel chest, is the most common congenital chest wall deformity. It affects approximately 1 in 400 to 1 in 1000 live births,[1] with males being 3-5 times more likely to be affected than females.[1] This structural anomaly can compress the heart and lungs, potentially leading to functional impairment. CT or MRI can both be used to assess pectus excavatum. The evaluation of pectus excavatum primarily utilizes the Haller index (HI) to determine the severity of sternal depression. A mild deformity is considered when HI values are between >2 and 3.2, moderate deformity is noted with HI between 3.2 and 3.5, and a severe deformity is indicated by an HI of >3.5. Patients typically require surgical correction if their HI values exceed 3.2, while normal values range between 2.0 and 3.0. If needed, pectus excavatum is treated surgically. The Nuss procedure is a minimally invasive surgical technique for pectus excavatum repair. This procedure involves the insertion of a curved substernal bar into the chest through 2 lateral thoracic incisions.

Keywords: thorax, sternum, congenital

Case Summary

An adolescent male presented to the chest wall deformity clinic with a visible pectus excavatum deformity.

Imaging Findings

Cardiac MRI (Figure 1) and chest CT (Figure 2) showed a severe pectus excavatum deformity with a Haller index (HI) of 10. The chest wall deformity was compressing the heart at the atrioventricular junction. The pectus deformity was treated by placing 2 pectus bars (Figure 3).

Diagnosis

Pectus excavatum

Discussion

Pectus excavatum, commonly known as sunken or funnel chest, is the most common congenital chest wall deformity, accounting for 90% of all such deformities in children. It affects approximately 1 in 400 to 1 in 1000 live births,[1] with males being 3-5 times more likely to be affected than females.[1] The deformity primarily results from an excessive growth of connective tissue, causing the sternum to invert. Depending on the rotation pattern of the sternum, pectus excavatum can be symmetrical or asymmetrical.[1] In either pattern, this structural anomaly can compress the heart and lungs, potentially leading to functional impairment.

In addition to its physical manifestations, pectus excavatum is frequently associated with syndromes, further complicating its clinical presentation. Notably, patients with pectus excavatum have a significantly higher propensity for concurrent connective tissue disorders; for instance, they are 16.7 times more likely to have Marfan syndrome compared with the general population (5% versus 0.3%).[2] Beyond Marfan syndrome, this deformity is linked with a variety of other congenital genetic disorders, including Ehlers-Danlos syndrome, Noonan syndrome, neurofibromatosis type 1, Turner syndrome, and autism spectrum disorder.[3]

Patients with pectus excavatum commonly report a range of symptoms that significantly impact their daily activities and quality of life. The most frequently reported symptoms include exercise intolerance, chest pain, and shortness of breath. Although exercise intolerance is prevalent, most patients do not exhibit cardiac symptoms at rest. This discrepancy can be attributed to the inhibition of cardiac return and the subsequent decrease in cardiac output during physical activity, which results from the anatomical compression of the chest.[1] Additionally, some patients may

Affiliations: Creighton University School of Medicine, Omaha, Nebraska (Pinkhasova); Department of Radiology, Phoenix Children's Hospital, Phoenix, Arizona (RB Towbin, Schaefer); Department of Radiology, Cincinnati Children's Hospital, University of Cincinnati College of Medicine, Cincinnati, Ohio (Morin, AJ Towbin).

Disclosures: The authors have no conflicts of interest to disclose. None of the authors received outside funding for the production of this original manuscript and no part of this article has been previously published elsewhere.

https://doi.org/10.37549/JPCR-26-0086

Figure 1. (A) Axial T2-weighted image from a cardiac MR showing a severe pectus excavatum deformity causing compression of the heart (arrow) at the right atrioventricular junction. (B) The maximal depth of the deformity was just below the chest where there was compression of the chest wall upon the left liver. (C) The Haller index is calculated by drawing the maximal internal transverse diameter of the chest (dashed line), divided by the minimal anteroposterior depth of the chest from the vertebral body to the sternum at the same level (solid line). In this patient, the Haller index was 10. (D) The depression index (DI) is calculated by drawing a line connecting the anterior aspect of the ribs (dashed line). A second line (solid line) is drawn measuring the depth from the first line to the deepest portion of the anterior sternum. Finally, a third line (orange line) is drawn measuring the width of the vertebral body on the same image. The DI is then calculated as the depth/width. In this patient, the DI was 0.63. (E) The correction index (CI) is calculated by first drawing a horizontal line (dashed line) along the anterior aspect of the vertebral body. A second line (solid line) is drawn from the posterior aspect of the sternum at its deepest point to the horizontal line. Finally, a third line (orange line) is drawn from the most anterior portion of the inner chest wall to the horizontal line. The CI is then calculated as a percentage using the formula (Length of orange line – Length of yellow line)/Length of orange line)×100%. In this patient, the CI was 52%. (F) The sternal torsion angle (STA) is measured by determining the angle between a true horizontal line outside the patient (dashed line) and a line along the anterior aspect of the sternum (solid line). In this patient, the STA was –21° counterclockwise.

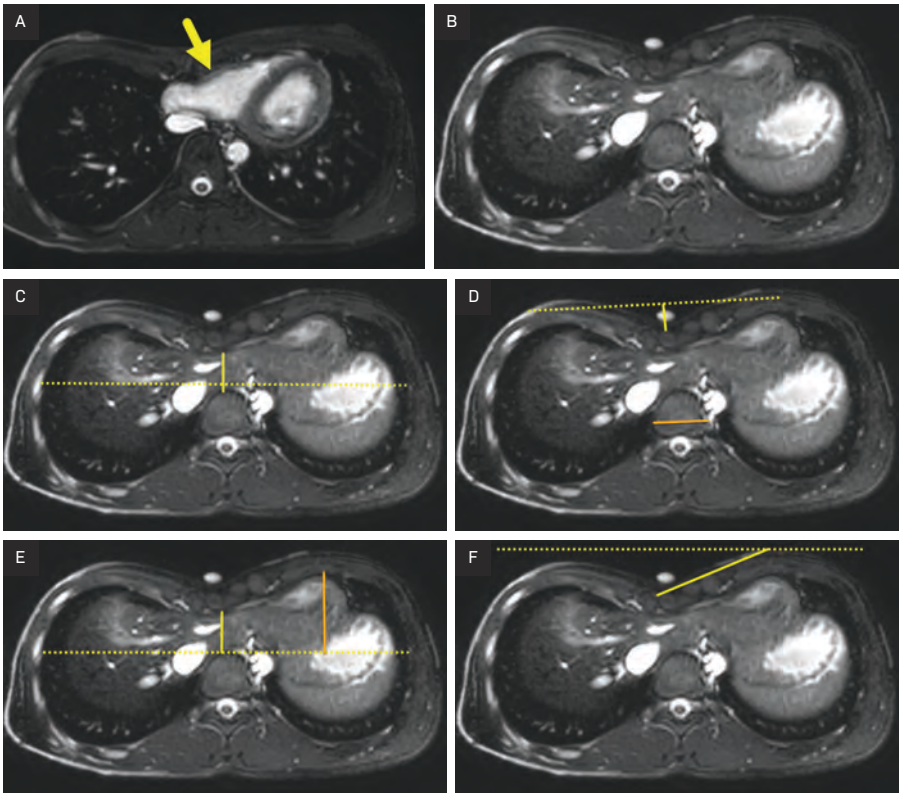

experience a persistent cough.[4] Furthermore, the distinctive physical appearance associated with pectus excavatum often affects the morale of adolescent patients, contributing to poor self-esteem and body image issues.

On physical examination, there is an inward displacement of the sternum and surrounding costal cartilages.[1] Sternal depression leads to a reduced sternovertebral distance and causes a leftward displacement of the heart. The cardiac displacement is often observable on an EKG as an axis deviation.[1] Pulmonary function tests may reveal decreased forced vital capacity, forced expiratory volume in one second, and the average forced expiratory flow rate between 25% and 75% of the vital capacity.[5]

CT or MRI can both be used to assess pectus excavatum. If CT is used, imaging can be focused to reduce radiation. If this strategy is used, the deepest portion of the sternal depression is identified using a Bb. This location is then used as the center point for imaging. The technologist can then expand the field of view 5 cm above and below the BB. If MR is performed, the whole chest can be imaged. The benefits of MRI include the lack of radiation and the ability to simultaneously assess cardiac function and the chest wall deformity, thus avoiding echocardiogram.[6]

Figure 2. Three-dimensional reconstruction from a chest CT highlighting the pectus excavatum deformity.

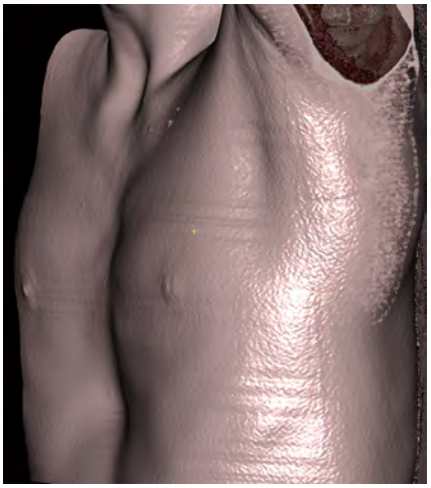

The evaluation of pectus excavatum primarily utilizes the HI to determine the severity of sternal depression. The HI is calculated by measuring the maximal internal transverse diameter of the chest from rib margin to rib margin, divided by the minimal anteroposterior depth of the chest from the vertebral body to the sternum at the same level. A mild deformity is considered when HI values are between >2 and 3.2, moderate deformity is noted with HI between 3.2 and 3.5, and a severe deformity is indicated by an HI of >3.5. Patients typically require surgical correction if their HI values exceed 3.2, while normal values range between 2.0 and 3.0.[7]

In addition to the HI, several other measures are used to describe the chest wall deformity. These indices guide surgical planning and provide supportive evidence to ensure that surgery is needed.

Correction index (CI): This measure evaluates the degree of sternal depression relative to the anterior chest wall. It is calculated by drawing a line (line a) from the posterior aspect of the sternum

Figure 3. (A) Frontal and (B) lateral chest radiographs after corrective surgery showing the placement of 2 bars correcting the pectus excavatum deformity.

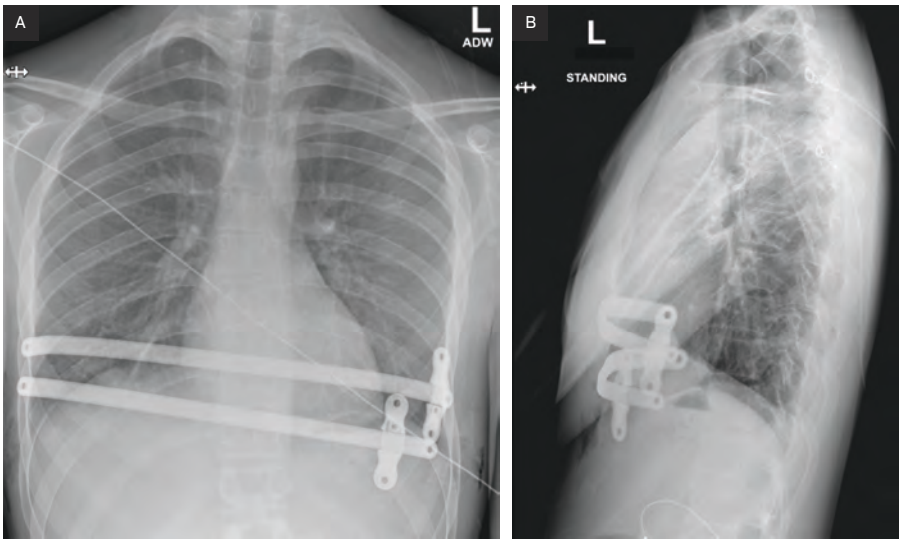

at its deepest point to a horizontal line drawn along the anterior aspect of the vertebral body. A second line (line b) is then drawn on the same image from the most anterior portion of the inner chest wall to the same horizontal line. The CI is then calculated as a percentage using the formula: (Length of line b − Length of line a)/Length of line b) × 100%. A CI greater than 10% is considered abnormal, indicating significant deformity that may benefit from surgical intervention.

Depression index (DI): The DI uses the vertebral body diameter as a baseline to assess the severity of the chest depression relative to an individual's size. It is calculated by identifying the deepest site of sternal depression. A line is then drawn connecting the anterior aspect of the ribs. A second line (depth) is drawn from the first line to the deepest portion of the anterior sternum. Finally, a third line is drawn measuring the width of the vertebral body on the same image. The DI is then calculated as the depth/width. A DI greater than 0.2 is abnormal, suggesting a notable inward depression of the sternum.

Sternal torsion angle (STA): The STA measures the angular deviation of the sternum, providing a quantitative assessment of the torsional deformation of the chest wall. This measure is particularly useful in surgical planning and assessing the asymmetry of the chest wall deformity. It is measured by determining the angle between a true horizontal line outside the patient and a line along the anterior aspect of the sternum. By convention, a right side-down sternal tilt is reported using negative numbers and described as counterclockwise, while a left-side down tilt is reported using positive numbers and described as clockwise.

If needed, pectus excavatum is treated surgically. The Nuss procedure is a minimally invasive surgical technique for pectus excavatum repair. This procedure involves the insertion of a curved substernal bar into the chest through 2 lateral thoracic incisions. The bar is carefully guided through the mediastinum using thoracoscopy and is typically removed after 2-4 years.[8] One of the major advantages of this approach is that it avoids the need for costal cartilage resection or sternal osteotomy, thereby reducing recovery time and postoperative complications.[9]

Eligibility for the Nuss procedure requires meeting at least 2 of the following 6 criteria:

1. Symptomatic manifestation of the deformity
2. Severe pectus excavatum deformity observable on physical examination
3. An HI >3.2
4. Pulmonary function tests showing restrictive or obstructive patterns
5. Evidence of cardiac compression or displacement
6. Significant impact on the patient's body image and self-esteem[8]

These criteria ensure that the procedure is reserved for patients who will most likely benefit from surgical intervention, taking into consideration both physical health impacts and psychological well-being.

A 2016 review demonstrated highly favorable outcomes for the Nuss procedure, with 98% of patients achieving excellent results, characterized by normal chest anatomy and minimal residual sternal depression.[8] Post-surgery, patients commonly experience significant improvements in cardiovascular function, including increased stroke volume and cardiac output, as well as gradual enhancements in pulmonary function following the removal of the substernal bar.[8]

Despite the high success rate, certain complications have been noted. Initially, bar displacements requiring surgical revision were reported at a rate of 3.7% and overcorrections occurred in approximately 3.1% of cases. To address these issues, refinements such as the incorporation of stabilizers and subcostal sutures have been implemented, substantially reducing the rate of bar displacement to 1%.[8] These adjustments have improved the procedure's safety and efficacy, further solidifying its role as a critical intervention for severe pectus excavatum.

Pectus excavatum, the most common congenital chest wall deformity, affects both physical health and psychological well-being.[10] It is characterized by inward displacement of the sternum, which, in severe cases, can compress the heart and lungs, leading to functional impairments. The condition is associated with various syndromes and can impact a patient's quality of life due to symptoms such as exercise intolerance and poor

https://doi.org/10.37549/JPCR-26-0086

body image. Diagnosis relies on imaging techniques such as CT and MRI, along with objective indices, including the HI, CI, DI, and STA, all of which help assess severity and guide surgical decision-making. When treatment is necessary, the Nuss procedure is the preferred corrective approach, improving both anatomical and functional outcomes. Despite potential complications, ongoing refinements in surgical techniques continue to enhance the procedure's safety and effectiveness.

Conclusion

Pectus excavatum, commonly known as sunken or funnel chest, is the most common congenital chest wall deformity. It affects approximately 1 in 400 to 1 in 1000 live births,[1] with males being 3-5 times more likely to be affected than females.[1] This structural anomaly can compress the heart and lungs, potentially leading to functional impairment.

CT or MRI can both be used to assess pectus excavatum. The evaluation of pectus excavatum primarily utilizes the HI to determine the severity of sternal depression. A mild deformity is considered when HI values are between >2 and 3.2, moderate deformity is noted with HI between 3.2 and 3.5, and a severe deformity is indicated by an HI of >3.5. Patients typically require surgical correction if their HI values exceed 3.2, while normal values range between 2.0 and 3.0. If needed, pectus excavatum is treated surgically. The Nuss procedure is a minimally invasive surgical technique for pectus excavatum repair. This procedure involves the insertion of a curved substernal bar into the chest through 2 lateral thoracic incisions.

References

1) Fokin AA, Steuerwald NM, Ahrens WA, Allen KE. Anatomical, histologic, and genetic characteristics of congenital chest wall deformities. *Semin Thorac Cardiovasc Surg*. 2009;21(1):44-57. doi:10.1053/j.semtcvs.2009.03.001

2) Behr CA, Denning N-L, Kallis MP, et al. The incidence of Marfan syndrome and cardiac anomalies in patients presenting with pectus deformities. *J Pediatr Surg*. 2019;54(9):1926-1928. doi:10.1016/j.jpedsurg.2018.11.017

3) Billar RJ, Manoubi W, Kant SG, et al. Association between pectus excavatum and congenital genetic disorders: a systematic review and practical guide for the treating physician. *J Pediatr Surg*. 2021;56(12):2239-2252. doi:10.1016/j.jpedsurg.2021.04.0164

4) Donato BB, Linnaus ME, Velazco CS, et al. Severe pectus excavatum with tracheal compression presenting with chronic cough. *J Pediatr Surg Case Rep*. 2018;33:14-16. doi:10.1016/j.epsc.2018.03.004

5) Kelly RE Jr, Obermeyer RJ, Nuss D. Diminished pulmonary function in pectus excavatum: from denying the problem to finding the mechanism. *Ann Cardiothorac Surg*. 2016;5(5):466-475. doi:10.21037/acs.2016.09.09

6) Birkemeier KL, Podberesky DJ, Salisbury S, Serai S. Limited, fast magnetic resonance imaging as an alternative for preoperative evaluation of pectus excavatum: a feasibility study. *J Thorac Imaging*. 2012;27(6):393-397. doi:10.1097/RTI.0b013e31822da1b6

7) Daunt SW, Cohen JH, Miller SF. Age-related normal ranges for the haller index in children. *Pediatr Radiol*. 2004;34(4):326-330. doi:10.1007/s00247-003-1116-1

8) Nuss D, Obermeyer RJ, Kelly RE. Nuss bar procedure: past, present and future. *Ann Cardiothorac Surg*. 2016;5(5):422-433. doi:10.21037/acs.2016.08.05

9) Nuss D, Kelly RE Jr. Minimally invasive surgical correction of chest wall deformities in children (Nuss procedure). *Adv Pediatr*. 2008;55:395-410. doi:10.1016/j.yapd.2008.07.012

10) Zuidema WP, Oosterhuis JWA, Zijp GW, et al. Early consequences of pectus excavatum surgery on self-esteem and general quality of life. *World J Surg*. 2018;42(8):2502-2506. doi:10.1007/s00268-018-4526-9

Fibrosing Mediastinitis

Eden Johnson, BS; Richard B. Towbin, MD; Jeffrey A. Towbin, MD; Alexander J. Towbin, MD; Jason N. Johnson, MD, MHS

Abstract

Fibrosing mediastinitis (FM) is a potentially destructive disease that affects mostly young patients who present with signs and symptoms related to obstructed mediastinal structures. Most granulomatous FM cases are unilateral and caused by histoplasmosis infection. Nongranulomatous FM is more diffuse and has varying causes but is thankfully rare. CT and MRI are key in the diagnosis and management of FM, vital to assessing the extent of mediastinal involvement, and essential for guiding either surgical or transcatheter therapy.

Keywords: thorax, mediastinum, infection

Case Summary

An adolescent male presented with chest pain and mild shortness of breath with activity. Physical exam showed normal vital signs, normal heart sounds, and breath sounds were clear to auscultation bilaterally.

Imaging Findings

Chest x-ray (Figure 1) showed right basilar atelectasis, trace right pleural effusion, and right middle lobe volume loss. Transthoracic echocardiogram (Figure 2) showed external compression of the proximal superior vena cava, right pulmonary artery, and right pulmonary veins from a mediastinal mass. Chest CTA (Figure 3) showed a partially calcified conglomerate right hilar mass causing near occlusion of the right pulmonary artery, right pulmonary veins, right mainstem bronchus, bronchus intermedius, right middle-lobe bronchus, and right lower lobe bronchus.

Diagnosis

Fibrosing mediastinitis (FM), granulomatous form from histoplasmosis infection.

The differential diagnosis of FM is other infections causing granulomas like tuberculosis, mycobacterial infections, and other fungal infections (aspergillosis and coccidioidomycosis). Most cases of granulomatous FM are unilateral and caused by histoplasmosis. Nongranulomatous causes of FM include sarcoidosis, autoimmune diseases (rheumatoid arthritis and lupus), radiation therapy, medications, and idiopathic conditions. Malignancies (lymphoma, thymoma, lung cancer, and metastatic cancers), amyloidosis, lymphangiomatosis, and granulomatosis with polyangiitis are also important differentials to consider.

Figure 1. Posterior-anterior chest x-ray with right basilar atelectasis, trace right pleural effusion, and right middle-lobe volume loss.

Discussion

FM or sclerosing mediastinitis is a rare disorder consisting of inflamed fibrous tissues within the mediastinum. Within the mediastinum are the heart, blood vessels, trachea, esophagus, lymph nodes, and the thymus.[1] These structures can all be subject to compression by the invasive fibrous tissues, resulting in pain and discomfort for patients diagnosed with this disorder. FM occurs in regions where fungal antigens have been seen to be associated with a fibrosing response within the body's immune system.[2] This response can be the result of the fungus *Histoplasma capsulatum* spreading within

Affiliations: University of Tennessee, Knoxville, Tennessee (E Johnson); Department of Radiology, Phoenix Children's Hospital, Phoenix, Arizona (RB Towbin); Heart Institute, Le Bonheur Children's Hospital, Memphis, Tennessee (JA Towbin, JN Johnson); Department of Radiology, Cincinnati Children's Hospital, University of Cincinnati College of Medicine, Cincinnati, Ohio (AJ Towbin).
Disclosures: The authors have no conflicts of interest to disclose. None of the authors received outside funding for the production of this original manuscript and no part of this article has been previously published elsewhere.

https://doi.org/10.37549/JPCR-26-0087

Figure 2. (A) Transthoracic echocardiogram color compare subcostal sagittal view. There is an anterior mass causing external compression of the superior vena cava (SVC). There is an increased flow gradient (8 mm Hg, normal 1-2 mm Hg) across the SVC in the area of external compression. RA, right atrium. (B) Transthoracic echocardiogram color Doppler parasternal short-axis view. There is minimal color flow to the right pulmonary artery (RPA) compared with the left pulmonary artery (LPA), supporting severe stenosis of the right pulmonary artery.

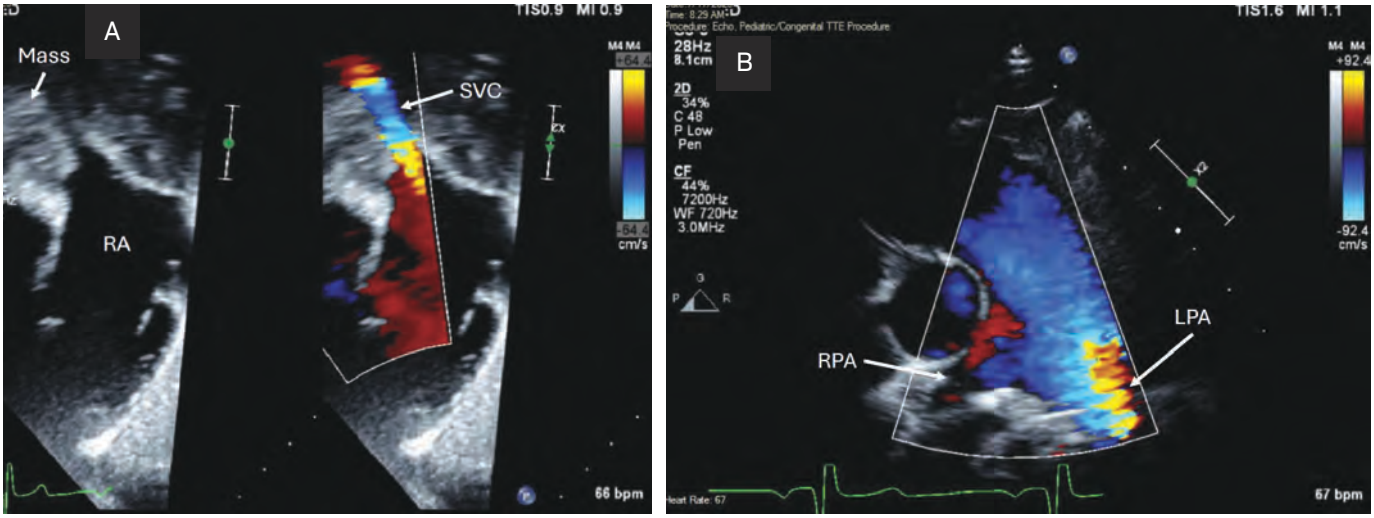

Figure 3. (A) Chest CTA axial plane. There is a large partially calcified conglomerate right hilar mass causing severe external compression of the superior vena cava (SVC) and moderate external compression of the right mainstem bronchus. LPA, left pulmonary artery. (B) Chest CTA axial plane. There is a large partially calcified conglomerate right hilar mass causing complete occlusion of the right pulmonary artery (RPA) just prior to the first-order branches. There is moderate external compression of the right mainstem bronchus (R Bronchus). L Bronchus, left mainstem bronchus; LPA, left pulmonary artery. (C) Chest CTA axial plane. There is a large partially calcified conglomerate right hilar mass causing complete occlusion of the right pulmonary veins. LA, left atrium; LPV, left pulmonary vein; LV, left ventricle; RV, right ventricle.

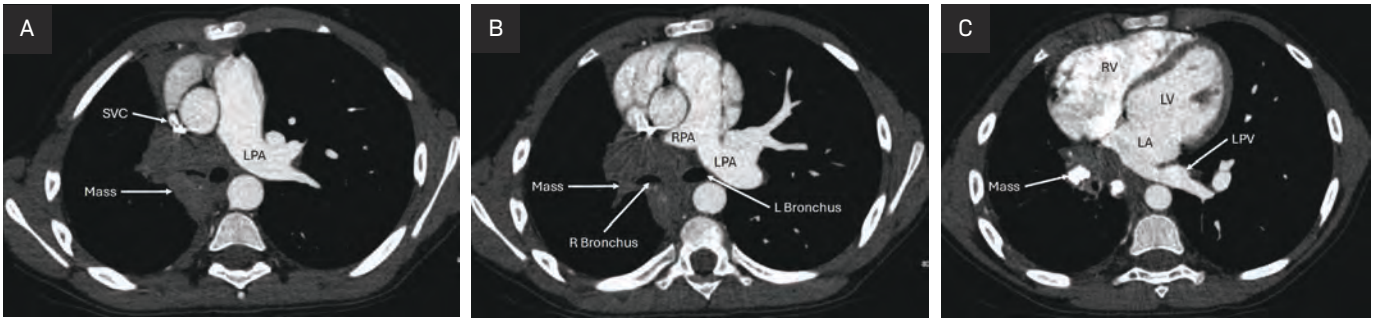

the mediastinum forming granulomas and is typically the most common cause in the United States.[3] The exact prevalence of FM is unknown as it typically occurs in regions where fungal infections are endemic, but not all patients experience the severity of FM.[4] Clinical cases of histoplasmosis infections mostly appear benign, with progression to FM rare.

Not all cases of FM are related to histoplasmosis. Other infections like tuberculosis and other fungal infections (aspergillosis and mucormycosis) can cause FM.[5] FM has also been reported in the setting of autoimmune diseases, rheumatic fever, radiation therapy, cancers, and certain drug therapy.[6] Patients with FM exhibit various symptoms, including pleuritic chest pain, cough, dyspnea, and hemoptysis commonly, and fever, tachycardia, and weight loss rarely. FM typically involves individuals from 20 to 40 years old but has been described in children to older adults as well and affects men and women equally. Radiologic findings exhibit signs of mediastinal widening, hilar mass, and calcifications.[6]

The appearance of FM on CT is variable depending upon the pattern of involvement. In the granulomatous or localized disease, there are mediastinal or hilar masses often with calcium deposition. Calcium deposition is common in FM associated with histoplasmosis infections. CT also clearly shows the airways and vascular structures that are affected by the hilar mass.[7] In the nongranulomatous or diffuse type, there is soft-tissue obliteration of normal fat planes that encases or invades surrounding structures. FM is seen by MRI as a heterogeneous, infiltrative mass of variable signal intensity on T1- and T2-weighted MR images.

The areas of decreased signal intensity represent calcium deposits, and increased signal intensity represents inflammation.[6] Partially calcified hilar masses that do not cause external compression of surrounding structures are routinely seen on CT and MRI studies in endemic regions and do not result in FM. These patients usually never develop FM and are just observed.

Overall, mortality of FM tends to be low, depending on the affected structures in the mediastinum.[4] Severe forms of FM can result in pulmonary hypertension and right heart failure that leads to higher mortality rates.[2] Mediastinal granulomas typically are benign but do result in a worse prognosis when lesions compress neighboring structures.[2] A mortality rate as high as 30% has been reported, but this likely reflects the more severe cases of FM with bilateral involvement and not localized hilar masses that are more common.[8]

Treatment of FM varies depending upon the presentation and severity of the disease. Treatment can range from observation to medical therapy with antifungals and steroids to procedural options (surgical debulking or stenting/balloon dilation of affected vessels).[4] As most cases of FM are related to histoplasmosis infection, antifungal therapy (ketoconazole) is often used first line with varying success.[9] Most cases of FM present well after active histoplasmosis infection and resultant inflammation has resolved, so steroid treatment has varying success as well.[1] Surgical debulking can be effective in unilateral disease but with varying success.[1,9,10] Currently, balloon dilation and/or stent angioplasty of affected vessels is utilized more than surgical debulking as a less invasive option.[1] The severity of external compression and ability to successfully re-cannulate affected vessels determines the decision to proceed with invasive options.

Conclusion

FM is a potentially destructive disease that affects mostly young patients who present with signs and symptoms related to obstructed mediastinal structures. Most cases of granulomatous FM are unilateral and caused by histoplasmosis infection. Nongranulomatous FM is more diffuse and has varying causes but is thankfully rare. CT and MRI are key in the diagnosis and management of FM, vital to assessing the extent of mediastinal involvement, and essential for guiding either surgical or transcatheter therapy.

References

1) Lin J, Jimenez CA. Acute mediastinitis, mediastinal granuloma, and chronic fibrosing mediastinitis: a review. *Semin Diagn Pathol*. 2022;39(2):113-119. doi:10.1053/j.semdp.2021.06.008

2) Peikert T, Colby TV, Midthun DE, et al. Fibrosing mediastinitis: clinical presentation, therapeutic outcomes, and adaptive immune response. *Medicine*. 2011;90(6):412-423. doi:10.1097/MD.0b013e318237c8e6

3) Jain N, Chauhan U, Puri SK, Agrawal S, Garg L. Fibrosing mediastinitis: when to suspect and how to evaluate?. *BJR Case Rep*. 2016;2(1):20150274. doi:10.1259/bjrcr.20150274

4) McNeeley MF, Chung JH, Bhalla S, Godwin JD. Imaging of granulomatous fibrosing mediastinitis. *AJR Am J Roentgenol*. 2012;199(2):319-327. doi:10.2214/AJR.11.7319

5) Lee JY, Kim Y, Lee KS, Chung MP. Tuberculous fibrosing mediastinitis: radiologic findings. *AJR Am J Roentgenol*. 1996;167(6):1598-1599. doi:10.2214/ajr.167.6.8956619

6) Rossi SE, McAdams HP, Rosado-de-Christenson ML, Franks TJ, Galvin JR. Fibrosing mediastinitis. *Radiographics*. 2001;21(3):737-757. doi:10.1148/radiographics.21.3.g01ma17737

7) Garin A, Chassagnon G, Tual A, Revel MP. CT features of fibrosing mediastinitis. *Diagn Interv Imaging*. 2021;102(12):759-762. doi:10.1016/j.diii.2021.05.013

8) Loyd JE, Tillman BF, Atkinson JB, Des Prez RM. Mediastinal fibrosis complicating histoplasmosis. *Medicine*. 1988;67(5):295-310. doi:10.1097/00005792-198809000-00002

9) Urschel HC Jr, Razzuk MA, Netto GJ, Disiere J, Chung SY. Sclerosing mediastinitis: improved management with histoplasmosis titer and ketoconazole. *Ann Thorac Surg*. 1990;50(2):215-221. doi:10.1016/0003-4975(90)90737-q

10) Dunn EJ, Ulicny KS Jr, Wright CB, Gottesman L. Surgical implications of sclerosing mediastinitis. a report of six cases and review of the literature. *Chest*. 1990;97(2):338-346. doi:10.1378/chest.97.2.338